2024, 21(10): 3266-3276
https://doi.org/10.21123/bsj.2024.8822
P-ISSN: 2078-8665 - E-ISSN: 2411-7986
Baghdad Science Journal

Radioactive Source-Detector System: Design and Monte Carlo Opinion

Zainab kareem Ali , ***Ali N. Mohammed*** *

Department of Physics, College of Education, Mustansiriyah University, Baghdad, Iraq.
*Corresponding Author.

Received 30/03/2023, Revised 23/10/2023, Accepted 25/10/2023, Published Online First 20/03/2024, Published 01/10/2024

Abstract

In the current research, a computer simulation program was designed and written according to the Monte Carlo method to serve as a virtual practical system instead of a real one. The program has been statistically, geometrically and numerically tested for virtual radioactive source-detector setup. The simulation program is carried out for NaI(Tl) detector, and once for Gieger-Muller counter, for a range of energy up to 10 MeV. The Law of Large Numbers and the Central Limit Theorem were used to test the accuracy and precision of the program's workflow and an indication of how the results are close to their averages and, statistically, how they tend to a normal distribution. Generally, results of a number of detector efficiency types showed a high agreement with published experimental and several global codes results within a percentage error of ~ 0.02-5% (i.e. the accuracy ~ 95-99.98%) and the significance level reflects the precise of the algorithm of simulation. The accurate and precise estimation of the current simulation gives it the desired reliability. The current simulation program also showed flexibility and effectiveness in designing any nuclear source-detector system and providing the relevant workers or experimenters with indicators that help in the optimal design of a system in terms of equipment and geometrical configuration with the least time. It may take a few seconds to a few minutes of execution time for a personal computer with normal specifications. Unlike laboratory experiments which may take from several minutes to several hours. In addition, it provides an ideal work environment that is completely free of radiation hazards. Also, the current simulation provides a deep understanding of the interactions that occur in a real physical practical system.

Keywords: Central limit theorem, Large numbers law, Monte Carlo simulation, NaI(Tl) detector efficiency, Radiation counting statistics.

Introduction

Designing and testing a particular detection system usually brings some financial costs and time considerations[1]. Numerical Simulation can be an effective and economical alternative tool. Monte Carlo simulation is a numerical simulation method that mimics physical phenomena and can be thought of as an 'experiment' carried out on a personal computer. Since Monte Carlo is a simulation of stochastic processes[2,3], therefore, it can be used for designing and analyzing radiation detectors. This is because detector responses are derivable from Measurable quantities such as particle flux or current densities, that can be interpreted as expected of a statistical system.

In nuclear and radiation physics, one of the main reasons to implement Monte Carlo simulation is that, in many practical cases, it is difficult to provide calibrated radioactive-sources that cover all energy ranges; furthermore, these sources are obviously limited regarding to their dimensions and compositions. With, by Monte Carlo technique, one can reproduce, flexibly, any experimental circumstances, whatever complicated[4]. Another clear advantage of this approach is the short computation time.

As can be done by experimental[5,6] or theoretical[7,8] approaches, Monte Carlo technique has been used in gamma detection techniques which have a fundamental role in the field of gamma-rays spectroscopy[9,10] applied in nuclear physics, radiation measurement of environmental samples radiation dosimetry[11-15], medical radiography[16], neutron activation analysis[17], well logging[18], and study of cosmic rays[19].

Monte Carlo simulation computer program, as a virtual setup, was designed and written to be used instead of a real experimental system. The achievements concerning time assumption and flexibility versus the complicated were verified. A number of statistical, geometrical and characteristic parameters concerning the detection system have been estimated.

Materials and Methods

The proposed configuration for the current simulation is shown in Fig. 1 including, a 'virtual', radioactive source and detector (for example type of NaI(Tl)), in the coordinates system. The source lies within the fixed dimensions system with Cartesian coordinate axes (x,y,z)[20] to determine the position of the source with respect to the axial z-axis.

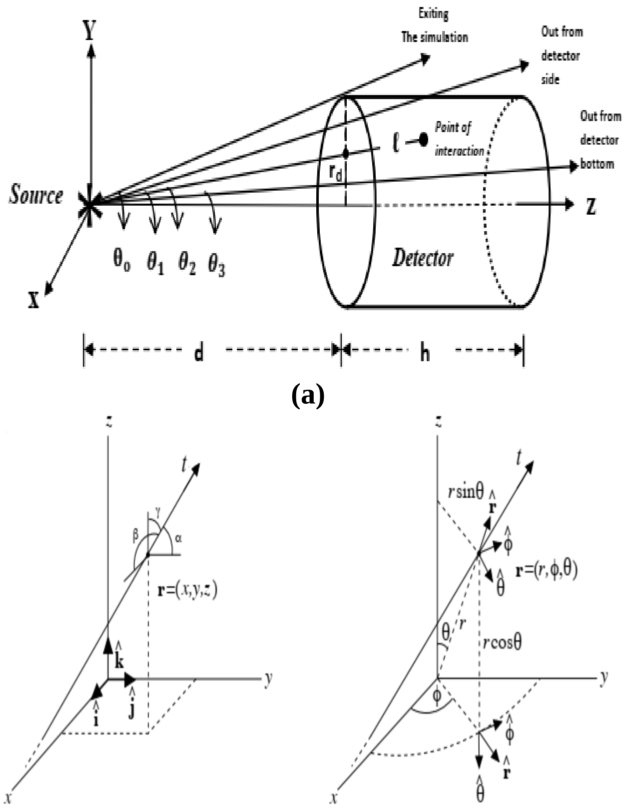

(a)

b1 **(b)** **b2**

Figure 1. The suggested design for the present source-detector systems simulation, the trajectory *t* represents a propagating "beam" of γ-ray that passes through point r in many of random directions.
(a) Fixed dimensions system and, (b) Reference dimensions system. Where, (b1) The Cartesian coordinate system (x, y, z) and, (b2) The Spherical coordinate system (r, θ, φ), where r is the radial distance from the origin, θ with the range $0 \leq \theta \leq \pi$ is the polar (or zenith) angle and φ with range $0 \leq \varphi \leq 2\pi$ is the azimuthal angle.

While the space outside of the source volume towards the detector lies within the reference dimensions system with spherical coordinate axes (r,θ,φ)[20] to follow the random geometric projections of emitted photons from the source on the planes of the detector and to determine the random probabilities of whether or not a photons they were to fall and be detected. The distance between the source and the detector can change. Based on the suggested configuration, a Fortran95 program for Monte Carlo simulation has been developed. It was designed and written to depict the interaction processes that occurred when the photon beam came into the detector, the results of which are that only the photons that are incident within a solid angle covered by the detector are to be impinging with the front face of the detector. These photons, later, are to be registered (counted) after satisfying a number of concern conditions as will be explained. These registered events allowed us to study "virtually" the characteristics of the experimental system concerning geometrical characteristics of a system. The present program is executed by Compaq Visual Fortran Professional edition 6.6.0, 2000 compiler package under windows 10.

The attenuation in the material of the radioactive source and in the air between the source and detector

2024, 21(10): 3266-3276
https://doi.org/10.21123/bsj.2024.8822
P-ISSN: 2078-8665 - E-ISSN: 2411-7986
Baghdad Science Journal

are neglected. The particles are transferred using the eq. 1[21]:

$$\vec{x} = \overrightarrow{x_o} + \vec{u}s \; \cdots\cdots\cdots 1$$

where: $\overrightarrow{x_o}$ is initial position, $\vec{x}$ is a new position with $\vec{u}$ direction and s is the distance that the particle travels before it intersects with a plane of a specific region.

In calculating particle transport in Monte Carlo as well as ray-tracing algorithms, a common problem is finding the distance a particle must travel in order to intersect a particular surface. Therefore the distribution function method can be used to sample the distributed photon path length. The probability function is given by Eq. 2[22]:

$$p(x) = \mu_l \, exp(-\mu_l x) \; \cdots\cdots\cdots \; 2$$

where: μ_l is the linear attenuation coefficient for a certain medium.

Briefly, the history of photons can be illustrated in the following algorithm:

1. Based on simple linear congruential generators (LCG)[21], generate two random numbers Rn_1 and Rn_2 into the interval (0, 1).

2. In fixed coordinates, using Eq. 1 to determine the random gamma emitting position from a radioactive source, with r_s Radius, (x_s,y_s,z_s)[22]:

$$x_s = r_{nx} + r_s \cos\theta_o \; \cdots\cdots\cdots 3a$$

$$y_s = r_s \sin\theta_o \; \cdots\cdots\cdots 3b$$

$$z_s = 0 \; \cdots\cdots\cdots 3c$$

where r_{nx} is off-axial location of source. Then a certain counter called emitting photon is increasing.

3. As in step 1, generate two random numbers Rn_3 and Rn_4 within range [0,1].

4. By using cosine sampling[21], Forced formulas have estimated the values of incident angles of photons on the front face of the detector[22],

$$\theta_i = \cos^{-1}\Big(\big((1 - Rn_3)\cos\theta_{min}\big) + (Rn_3 \cos\theta_{max})\Big) \; \cdots\cdots\cdots \; 4a$$

$$\varphi_i = \Big(\big((1 - Rn_4)\varphi_{min}\big) + (Rn_4 \varphi_{max})\Big) \; \cdots\cdots\cdots \; 4b$$

5. In the reference dimensions system, Fig. 1 b2 sampling Eq. 1 in spherical coordinates to locate the intersection point of random gamma photon path with the front face of the detector $\left(x_s^{df}, y_s^{df}, z_s^{df}\right)$,[22]

$$x_s^{df} = x_s + t_s^{df} \sin\theta_i \cos\varphi_i \; \cdots\cdots\cdots \; 5a$$

$$y_s^{df} = y_s + t_s^{df} \sin\theta_i \sin\varphi_i \; \cdots\cdots\cdots \; 5b$$

$$z_s^{df} = z_s + t_s^{df} \cos\theta_i \; \cdots\cdots\cdots \; 5c$$

6. Calculate the spherical projection radius of a gamma-ray on the front detector face r_{df}, where:

$$r_{df} = \left(x_s^{df} + y_s^{df}\right)^{1/2} \; \cdots\cdots\cdots 6$$

7. If $r_{df} > r_d$, this means that the radius of the spherical projection of the photon is greater than the radius of the front face of the detector. Then the photon was rejected, a certain counter called non -incident is increasing, and come back to step 1, else a certain counter called incident photon is increasing, then continue.

8. Generate one random number $Rn_5 : 0 \leq Rn_5 \leq 1$

9. Solve the probability function[22], Eq. 2, to determine the free path-length of gamma photon within/not the active medium of detector gives:

$$l_{f.p.} = \frac{1}{\mu_l} \ln(1 - Rn_5) \; \cdots\cdots\cdots \; 7$$

10. From steps (5 and 9), estimate the photon interaction position location within the detector, that is, (x_d^w, y_d^w, z_d^w), then[22]:

$$x_d^w = x_s + \left(l_{f.p.} + t_s^{df}\right) \sin\theta_i \cos\varphi_i \; \cdots\cdots\cdots \; 8a$$

$$y_d^w = y_s + \left(l_{f.p.} + t_s^{df}\right) \sin\theta_i \sin\varphi_i \; \cdots\cdots\cdots \; 8b$$

$$z_d^w = z_s + \left(l_{f.p.} + t_s^{df}\right) \cos\theta_i \; \cdots\cdots\cdots \; 8c$$

11. Calculate the spherical projection radius of a gamma-ray on the detector planes, r_{dw}. Where:

$$r_{dw} = (x_d^w + y_d^w)^{1/2} \; \cdots\cdots\cdots 9$$

12. With exception when $r_{dw} < r_d$ and $d_{sd} < z_d^w < (d_{sd} + h_d)$, the photon must be rejected and a certain counter called unregistered photons are increasing, then come back to step 1, otherwise a

2024, 21(10): 3266-3276
https://doi.org/10.21123/bsj.2024.8822
P-ISSN: 2078-8665 - E-ISSN: 2411-7986

certain counter called registered photons are increasing, then continue.

13. Classification of the registered photon according to the type of interaction (photo-electric, Compton scattering or pair production) depending on the probability of occurrence of that interaction.
14. Repeat the above steps of the algorithm by the number of emitted photons from the radioactive source.
15. Ordering the results in particular files.

The total efficiency of the detector was estimated by comparing the number of registered photons and those that were emitted from the source. While, the intrinsic efficiency was estimated by the ratio of registered photons number to those that hit the front face of the detector. The geometric efficiency was estimated by comparing the number of photons that hit the front face of the detector and those that were emitted from the source.

The values of mass attenuation coefficients for the active medium of detector were calculated using the XCOM program[23].

For more Accurate validation, GM-counter system (type ABG, CAT: PA1885-020-030) as shown in Fig. 2 was used to validate, experimentally, some findings of the present simulation.

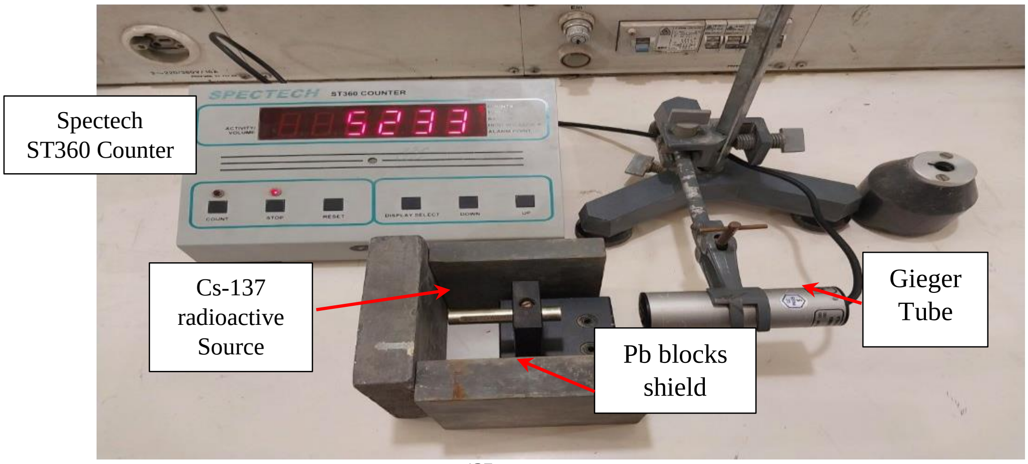

Figure 2. Uncovered (to illustration) ^{137}Cs radioactive source- GM counter configuration.

Results and Discussion

The random nature of radiation interaction with matter must be explained and interpreted according to probabilistic terms. Two of the main results in probability: are the Law of Large Numbers (LLN)[24] and the Central Limit Theorem (CLT)[24]. Both are related to sums of independent random varibles[6] that are included in the above algorithm. So, to complete the calculations with an accurate estimation of the value to be calculated, it must be re-implemented for a suitable large number of photon histories based on the LLN. Fig. 3. Exhibits a smaller number of trials for 10, 10^2 and 10^3 do not effectively estimate value conformity with a standard or observed value (one of values of Hoang[25]). While, the result of 10^4 and 10^5 trials produce a values are close to observed value. Concern 10^6 trials, the resultant are the closest with the smallest percentage error rate and highest accuracy.

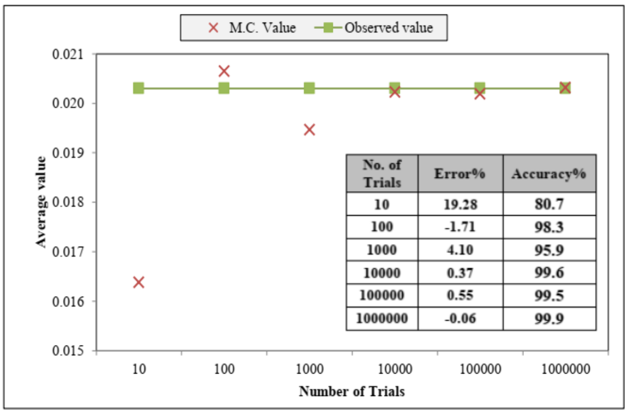

No. of Trials	Error%	Accuracy%
10	19.28	80.7
100	-1.71	98.3
1000	4.10	95.9
10000	0.37	99.6
100000	0.55	99.5
1000000	-0.06	99.9

Figure 3. A clarification of the law of large numbers using a particular run of the simulation.

These accuracy values refer to how Monte Carlo values get closer to the observed values up to 99.9%. However this test is insufficient to assess the

2024, 21(10): 3266-3276
https://doi.org/10.21123/bsj.2024.8822
P-ISSN: 2078-8665 - E-ISSN: 2411-7986
Baghdad Science Journal

performance of present simulation, because these values are based, in their calculation, on independent random variables. Consequently, besides the LLN, the CLT is considerably useful in precisely predicting the characteristics of these random variables and how they are distributed.

The experimental curve in Fig. 4 is the result of statistical repetitions of series of one hundred 1 minute counts of a Cs-137 source made with G-M laboratory counter set up which is shown in Fig. 2.

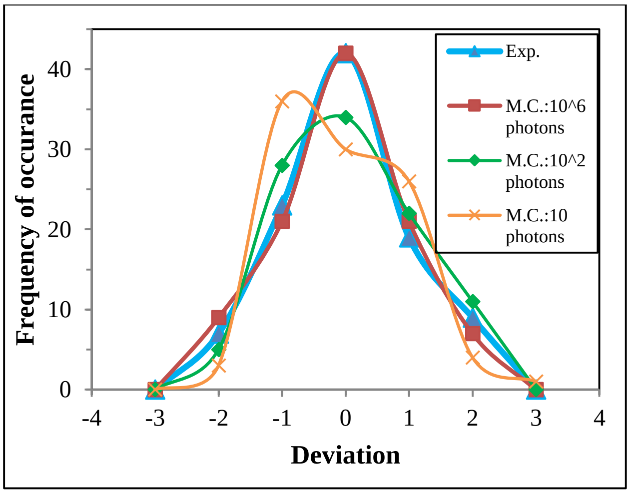

Figure 4. Experimental and simulated frequency distrbution curves.

While , the simulated curves in Fig.4 are the result of a series of one hundred 10, 10^2 and 10^6 history of photons for 662 keV that was executed to mimic the experimental setup that is shown in Fig. 2. The distribution curve of 10 history of photons is not normal, right another hump is formed. As for the curve of 100 history of photons is not precise enough to be normal. While the identical is clear between the experimental and simulated 10^6 history of photons curves and the variation between them is, axiomatically, due to random error introduced by radionuclide decay that is a randomly varying quantity. Therefore, repetition of more measurements, the measurements tend to be a normal distribution, as stated in the central limit theorem. Thats is, the values close to the expected value are more frequent than values that are far from them.

The average value for the results of series of 1 minute counts of a Cs-137 source made with G-M counter was 1940 C/1mint. with 40.4 of standard deviation and chi square (χ^2) 24.43. It took about 1.5 hours. Whereas for a series of one hundred 10^6 history of photons for 662 keV, the average was 250196 count with 449.5 of standard devaition and chi square 79.942. It took about 5 minutes. From the table of χ^2 values, the experimental and simulated significance level was 0.706 and 0.77 respectively. This indicates that the results reflect feasible instrument operation and the precision of the performance of the measurement system and the algorithm of simulation. The accurate and precise estimation of the current simulation gives it the desired reliability.

Fig. 5 depicts an additional representation of the total and partial attenuation coefficients for γ-rays, which were obtained through the current simulation of a 3"×3" NaI(Tl) detector at specific energies of a radioactive source. The attenuation coefficient, in probabilistic terms, describes how radiation interacts with matter. As a function of energy, Fig. 5 and Fig. 6 are identical.

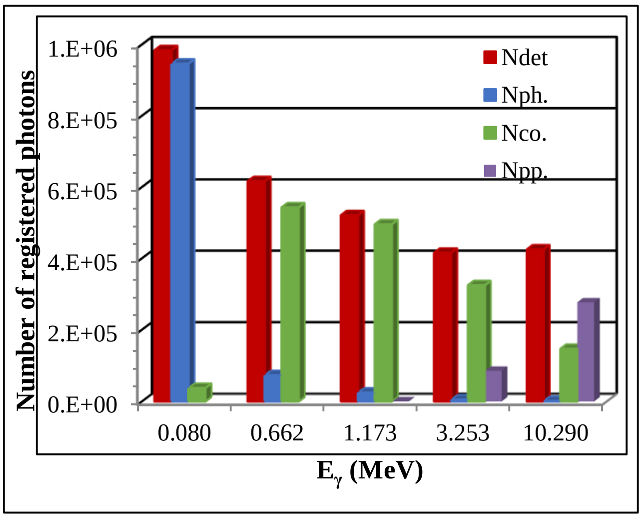

Figure 5. Comparing the number of detected photons that interact by photoelectric, Compton scattering and pair production effects at particular energy.

2024, 21(10): 3266-3276
https://doi.org/10.21123/bsj.2024.8822
P-ISSN: 2078-8665 - E-ISSN: 2411-7986

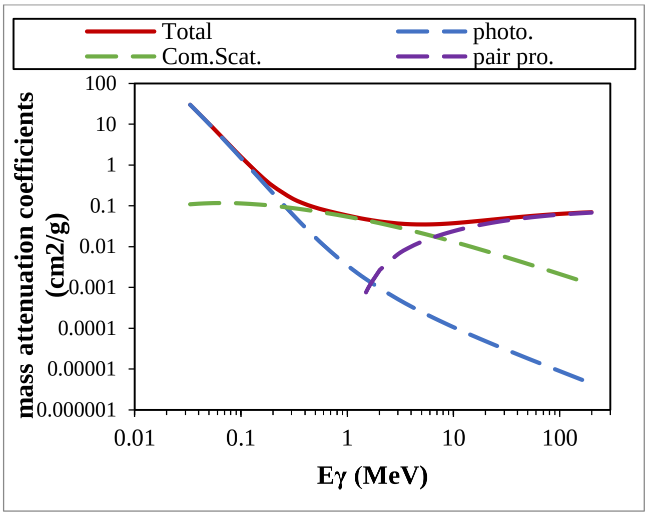

Figure 6. Total and partial mass attenuation coefficients of NaI(Tl) detector material.

Fig.7 shows the dependence of the registered count by detector versus the distance between the radioactive source and detector face (D_{sd}) for varied volume values of NaI(Tl) detector. When D_{sd} increases, the registered count decreases, and after passing through minimum, then it increases again. Since mean free path length of gamma rays is the inverse of the total attenuation coefficient as shown in Fig. 8. Therefore, as a function of geometry, Fig. 7 is upside down to Fig. 8 and vice versa. Similar results have been reported by Hoang [25] , Urkiye [26], Ogundare [27] and Jehouani [28].

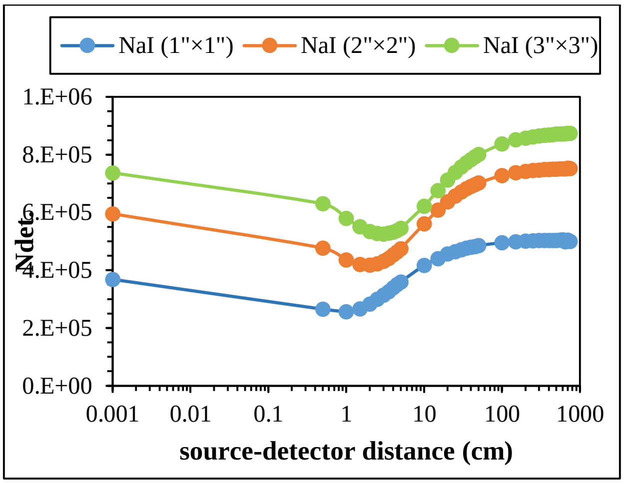

Figure 7. Variation of the registered count rate of different size of NaI(Tl) detectors as a function of source to detector distance for 662 keV of gamma rays.

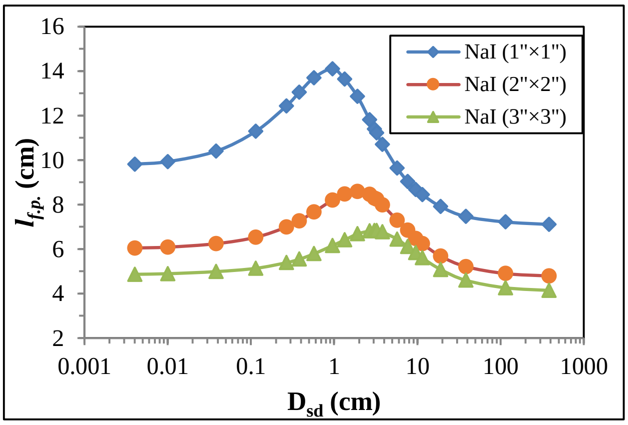

Figure 8. Mean free path length of various volume NaI(Tl) detectors as a function of Source-to-Detector distance at 662 keV of gamma rays.

Varying types of efficiency, as numerical factors, were mimicked to validate the present simulation. The outcomes, tabulated compared with published results [26] for For 2″×2″ of NaI(Tl) detector at particular distances 0.001, 5,10 and 15 cm for different energies 150-3000 keV as shown in Table 1. The comparison exhibits high agreement within a percentage error of ~ 0.02-5%. For further distances between the source and detector, the program has been implemented as it showed a clear match whether with the experimental or calculated results as shown in Table 2.

Table 1. For 2″×2″ of NaI(Tl) detector, Total, intrinsic and geometric efficiency comparison at particular distances for different energies.

	D (cm)	comparison	Energy (keV) 150	200	300	400	500	600	661	800	1000	1332	2000	3000
Total efficiency	0.001	ref.25	0.4988	0.4842	0.4192	0.3658	0.3318	0.3074	0.294	0.2738	0.2509	0.2295	0.1964	0.1793
		present M.C.	0.4987	0.4835	0.419	0.3665	0.33127	0.3091	0.297	0.2768	0.253	0.2243	0.1861	0.177
		error %	**0.02**	**0.14**	**0.05**	**0.19**	**0.16**	**0.55**	**1.02**	**1.10**	**0.84**	**2.27**	**5.24**	**1.28**
	5	ref.25	0.0476	0.0435	0.0363	0.0315	0.0285	0.0267	0.0255	0.0238	0.0219	0.02	0.0174	0.0157
		present M.C.	0.0478	0.0434	0.03635	0.0317	0.0287	0.0268	0.0259	0.0241	0.0221	0.01973	0.01637	0.01564
		error %	**0.42**	**0.23**	**0.14**	**0.63**	**0.70**	**0.37**	**1.57**	**1.26**	**0.91**	**1.35**	**5.92**	**0.38**
	10	ref.25	0.0141	0.0133	0.0117	0.0104	0.0096	0.0088	0.0086	0.0081	0.0074	0.0067	0.0059	0.0054
		present M.C.	0.0143	0.0134	0.01172	0.01044	0.00956	0.00899	0.00868	0.00811	0.00749	0.0067	0.0056	0.00534
		error %	**1.42**	**0.75**	**0.17**	**0.38**	**0.42**	**2.16**	**0.93**	**0.12**	**1.22**	**0.03**	**5.08**	**1.11**
	15	ref.25	0.0065	0.0064	0.0056	0.0051	0.0046	0.0044	0.0042	0.004	0.0037	0.0033	0.0029	0.0027
		present M.C.	0.00657	0.00628	0.00561	0.00508	0.00468	0.00441	0.00428	0.00402	0.00372	0.00334	0.00281	0.00268
		error %	**1.08**	**1.88**	**0.18**	**0.45**	**1.74**	**0.23**	**1.90**	**0.50**	**0.54**	**1.21**	**3.10**	**0.70**
Intrinsic efficiency	0.001	ref.25	0.998	0.9688	0.8387	0.7318	0.6639	0.615	0.5882	0.5477	0.5019	0.4591	0.393	0.3587
		present M.C.	0.9974	0.9672	0.8381	0.7331	0.6625	0.6183	0.5953	0.5536	0.507	0.4487	0.3723	0.354
		error %	**0.06**	**0.17**	**0.07**	**0.18**	**0.21**	**0.54**	**1.21**	**1.08**	**1.02**	**2.27**	**5.27**	**1.31**
	5	ref.25	0.8805	0.7999	0.6673	0.5816	0.529	0.4908	0.4699	0.4384	0.4024	0.3693	0.3189	0.2905
		present M.C.	0.8762	0.7969	0.6663	0.5823	0.5266	0.4929	0.4752	0.42	0.4069	0.3623	0.301	0.2876
		error %	**0.49**	**0.38**	**0.15**	**0.12**	**0.45**	**0.43**	**1.13**	**4.20**	**1.12**	**1.90**	**5.61**	**1.00**
	10	ref.25	0.9233	0.8656	0.753	0.6747	0.6158	0.5747	0.555	0.5189	0.4793	0.4415	0.3829	0.3514
		present M.C.	0.9212	0.8644	0.7545	0.673	0.6164	0.5798	0.56	0.5237	0.4842	0.4332	0.3626	0.3458
		error %	**0.23**	**0.14**	**0.20**	**0.25**	**0.10**	**0.89**	**0.90**	**0.93**	**1.02**	**1.88**	**5.30**	**1.59**
	15	ref.25	0.9451	0.904	0.8056	0.7228	0.6638	0.627	0.5995	0.5662	0.5219	0.4803	0.4174	0.3843
		present M.C.	0.9428	0.9002	0.8029	0.7237	0.6662	0.6272	0.6081	0.57	0.5275	0.4741	0.3979	0.3802
		error %	**0.24**	**0.42**	**0.34**	**0.12**	**0.36**	**0.03**	**1.43**	**0.67**	**1.07**	**1.29**	**4.67**	**1.07**
Geometric effi	0.001	ref.25	0.4998	0.4998	0.4998	0.4998	0.4998	0.4998	0.4998	0.4998	0.4998	0.4998	0.4998	0.4998
		present M.C.	0.49999	0.49999	0.49999	0.49999	0.49999	0.49999	0.49999	0.49999	0.49999	0.49999	0.49999	0.49999

2024, 21(10): 3266-3276
https://doi.org/10.21123/bsj.2024.8822
P-ISSN: 2078-8665 - E-ISSN: 2411-7986

ciency		**error %**	**0.038**	**0.038**	**0.038**	**0.038**	**0.038**	**0.038**	**0.038**	**0.038**	**0.038**	**0.038**	**0.038**	**0.038**
	5	ref.25	0.0541	0.0544	0.0543	0.0542	0.0539	0.0543	0.0542	0.0542	0.0544	0.0543	0.0545	0.0542
		present M.C.	0.0545	0.0545	0.0545	0.05453	0.0545	0.0545	0.0545	0.0545	0.05448	0.05446	0.0544	0.0544
		error %	**0.74**	**0.18**	**0.37**	**0.61**	**1.11**	**0.37**	**0.55**	**0.55**	**0.15**	**0.29**	**0.18**	**0.37**
	10	ref.25	0.0153	0.0154	0.0155	0.0154	0.0156	0.0153	0.0155	0.0155	0.0154	0.0153	0.0154	0.0153
		present M.C.	0.01554	0.01554	0.01553	0.0155	0.01551	0.0155	0.0155	0.01549	0.01548	0.01546	0.01543	0.01543
		error %	**1.57**	**0.91**	**0.19**	**0.65**	**0.56**	**1.31**	**0.00**	**0.06**	**0.52**	**1.05**	**0.19**	**0.85**
	15	ref.25	0.0069	0.0071	0.007	0.007	0.0069	0.0071	0.007	0.007	0.007	0.007	0.007	0.007
		present M.C.	0.00697	0.00698	0.00699	0.00701	0.00703	0.00704	0.00705	0.00705	0.00705	0.00705	0.00705	0.00705
		error %	**1.01**	**1.69**	**0.14**	**0.20**	**1.88**	**0.85**	**0.71**	**0.71**	**0.71**	**0.71**	**0.71**	**0.71**

Table 2. Variation of the total efficiency for a 3″× 3″ NaI(Tl) detector respect to point source of 662 keV located at particular distance from the front face and on the symmetric axis of detector.

d(cm)	**TEF**			**ERROR%**	
	Present M.C.	**Cal.[22]**	**Exp.[22]**	**M.C. vs. Cal.**	**M.C. vs. Exp.**
10	0.020483	0.02004	0.02053	2.16	0.23
15	0.010478	0.01024	0.01008	2.27	3.80
20	0.00626	0.0062	0.00594	0.96	5.11
25	0.00418	0.00415	0.00404	0.72	3.35
30	0.003004	0.00297	0.00294	1.13	2.13
35	0.002259	0.00223	0.0022	1.28	2.61
40	0.001776	0.00174	0.00175	2.03	1.46
45	0.001418	0.00139	0.00142	1.97	0.14
50	0.001164	0.00114	0.00124	2.06	6.53

To demonstrate the effect of the source dimensions, the simulation was carried out for a radiant source with a disk shape. The results were compared with the published results of the international code Geant4 based GATE simulation program[29], which clearly showed quite well congruence, see Fig. 9.

Another Validation was implementing the present simulation to scrutinize the detection efficiency versus different $2R_d/H_d$ ratio of NaI(Tl) detectors, so that the volume of detector remains fixed. The incident monoenergetic energies of γ-rays are 0.662, 1.331 and 4.438 MeV, experimentally, emitted from ^{137}Cs, ^{60}Co and ^{241}Am radioactive sources respectively [30]. As shown in Fig. 10, the result reveals that the detector efficiency dependent on the mentioned ratio of the NaI(Tl) detector and the incident energy of γ-photon. At a very low of $2R_d/H_d$, the total detector efficiency increases rapidly and tends to be stable while the intrinsic of which is on the contrary. Anyway, the ratio from 1-2, (i.e. with an average 1.5, matching with ref.30) is an interesting and meaningful point. It is valuable to design detectors for detecting γ-rays that have optimal dimensions.

2024, 21(10): 3266-3276
https://doi.org/10.21123/bsj.2024.8822
P-ISSN: 2078-8665 - E-ISSN: 2411-7986

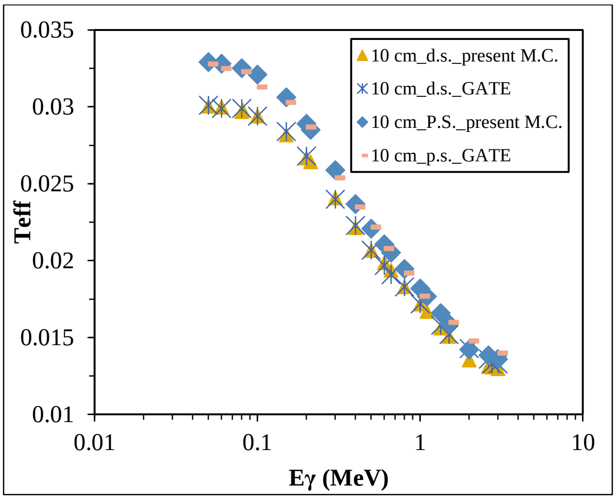

Figure 9. Total efficiency as a function of γ-ray comparison for point and disc radioactive source (p.s. and d.s. respectively).

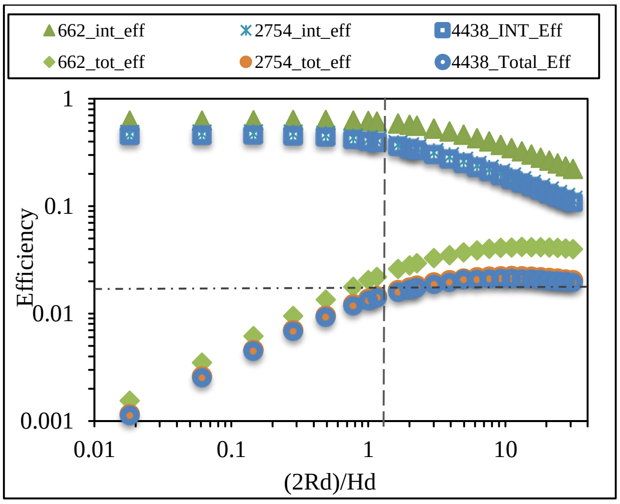

Figure 10. Intrinsic and total efficiency as a function of diameter to height ratio of 3″× 3″ NaI(Tl) detector at different values of γ-ray energy.

Conclusion

For the radioactive source-detector setup, Monte Carlo simulation computer program was designed, written and validated to be used instead of the real experimental system. Subsequently, the current works supplies are better to use provide with useful tool for γ-ray spectroscopy and fashions a good procedure for credible computations in lieu of the routine of laboratory or experimental measurements. Wherefore, one can sock away time by averting the calibration of practical setup for every geometry concerned. Significantly reducing radiation risks and in less time, the current simulation is a good turn for the experimenter to achieve the best and most suitable geometry of setup. Also, Monte Carlo simulation is a viable tool to design the optimal dimensions of detector for detecting of γ-rays.

Authors' Declaration

- Conflicts of Interest: None.
- We hereby confirm that all the Figures and Tables in the manuscript are ours. Furthermore, any Figures and images, that are not ours, have been included with the necessary permission for re-publication, which is attached to the manuscript.
- Ethical Clearance: The project was approved by the local ethical committee at Mustansiriyah University.

Authors' Contribution Statement

A.N.M and Z. K. A. conceived and designed the study, acquired the data, analyzed and interpreted the results and wrote the manuscript.

References

1. Fielding AL. Monte Carlo techniques for radiotherapy applications I: introduction and overview of the different Monte Carlo codes. J Radiother Pract. 2023; 22(e80): 1–6. https://doi.org/10.1017/S1460396923000079
2. Shapiro A. Monte Carlo Sampling Approach to Stochastic Programming. ESAIM: Proceedings, December 2003; 13: 65-73. https://doi.org/10.1051/proc:2003003
3. Gobet E. Monte Carlo Methods and Stochastic Processes From Linear to Non Linear. CRC Press, Taylor & Francis Group, LLC, 2016. https://doi.org/10.1080/14697688.2024.2310568
4. Paxton P, Curran PJ, Bollen KA, Kirby J, Chen F. Monte Carlo Experiments: Design and Implementation. Struct Equ Modeling: A Multidiscip J. 2001; 8(2): 287-312. https://doi.org/10.1207/S15328007SEM0802_7

5. Hameed BS, Kaddoori FF, Fzaa WT. Concentrations and Radiation Hazard Indices of Naturally Radioactive Materials for Flour Samples in Baghdad Markets. Baghdad Sci J. 2021; 18(3): 649-654. https://doi.org/10.21123/bsj.2021.18.3.0649
6. Kim J, Park K, Hwang J, Kim H, Kim J, Kim H, et al. Efficient design of a Ø2 × 2 inch NaI(Tl) scintillation detector coupled with a SiPM in an aquatic environment. Nucl Eng Technol. 2019; 51: 1091-1097. https://doi.org/10.1016/j.net.2019.01.017
7. Pepperosa A, Remetti R, Perondi F. ARMAX Forecast Model for Estimating the Annual Radon Activity Concentration in Confined Environment by Short Measurements Performed by Active Detectors. Int J Environ. Res. Public Health. 2022; (19): 5229. https://doi.org/10.3390/ijerph19095229
8. Zambonino SS, Barahona T, Roque S. Simulation of a HPGe Detector with GEANT4. Rev Politéc.. 2023; 50(2): 7-14. https://doi.org/10.33333/rp.vol50n2.01
9. Akkurt İ, Waheed F, Akyildirim H, Gunoglu K. Performance of NaI(Tl) detector for gamma-ray spectroscopy. Ind J Phys.. 2022; 96: 2941–2947. https://doi.org/10.1007/s12648-021-02210-1
10. Demir N, Kuluöztürk ZN. Determination of energy resolution for a NaI(Tl) detector modeled with FLUKA code. Nucl Eng Technol. 2021; 53: 3759-3763. https://doi.org/10.1016/j.net.2021.05.017
11. Pilakouta M, Pappa FK, Patiris DL, Tsabaris C, Kalfas CA. A methodology for expanding the use of NaI(Tl) based spectrometry in environmental radioactivity measurements. Appl. Radiat. Isot.. 2018; 139: 159-168. https://doi.org/10.1016/j.apradiso.2018.04.032
12. DePaiva JDS, Sousa EE, DeFarias EEG, DoCarmo AM, Filho CAS, De Franc EJ. Applied tools for determining low-activity radionuclides in large environmental samples. J Radioanal Nucl Chem. 2015; 306(3): 631-636. https://doi.org/10.1007/s10967-015-4219-x
13. Hinrichsen Y, Finck R, Martinsson J, Rääf C. Monte-carlo simulations of external dose contributions from the surrounding ground areas of residential homes in a typical northern european suburban area after a radioactive fallout scenario. Sci Rep. 2020; 10: 14764. https://doi.org/10.1038/s41598-020-71446-4
14. Baldoncini M, Albéri M, Bottardi C, Chiarelli E, Raptis KGC, Strati V, et al. Investigating the potentialities of Monte Carlo simulation for assessing soil water content via proximal gamma-ray spectroscopy. J Environ Radioact. 2018; 192: 105-116. https://doi.org/10.1016/j.jenvrad.2018.06.001
15. Külahci F, Aközcan S, Günay O. Monte Carlo simulations and forecasting of Radium-226, Thorium-232, and Potassium-40 radioactivity concen-trations. J Radioanal Nucl Chem.. 2020; 324(1): 55-70. https://doi.org/10.1007/s10967-020-07059-y
16. Kyriakou I, Sakata D, Tran HN, Perrot Y, Shin WG, Lampe N, et al. Review of the Geant4-DNA Simulation Toolkit for Radiobiological Applications at the Cellular and DNA Level. Cancers. 2022; 14: 35. https://doi.org/10.3390/cancers14010035
17. Gao Y, Jiaming L, Jichen L, Liu L. Simulation of the cement measurement based on the pulse DT neutron generator: A Monte Carlo study. PLoS One, 2021. https://doi.org/10.1371/journal.pone.0252078
18. Niu F. Application of position sensitive detector in nuclear well logging tools. PhD. Thesis. Simon Fraser University, Canada. 2020.
19. Sarkar R, Roy A, Chakrabarti S. Simulation of Cosmic Rays in the Earth's Atmosphere and Interpretation of Observed Counts in an X-ray Detector at Balloon Altitude Near Tropical Region. Adv Space Res.. 2020; 1: 189-197. https://doi.org/10.1016/j.asr.2019.09.046
20. Churchill CW. Radiative transfer. New Mexico State University. Chap 4: 2009. https://doi.org/10.1007/978-3-030-95247-1
21. Bielajew AF. Fundamentals of the Monte Carlo method for neutral and charged particle transport. The University of Michigan. 2020.
22. Ljungberg M, Strand SE, King MA. Monte Carlo Calculations in Nuclear Medicine: Applications in Diagnostic Imaging. IOP Publishing Ltd 1998 https://doi.org/10.1201/b13073
23. Berger MJ, Hubbell JM. XCOM Program V.3.1: Photon Cross Sections Database. NIST standard reference database. 1999. https://dx.doi.org/10.18434/T48G6X
24. Rubinstein RY, Kroese DP. Simulation and the Monte Carlo Method. 3rd ed., John Wiley & Sons. Inc., 2017. https://doi.org/10.1002/9781118631980
25. Tam HD, Thanh TT, Tao CV. Evaluation of the total and intrinsic efficiencies of a 3 in × 3 in NaI(Tl) crystal by using the hybrid Monte Carlo method. J Sci Technol Dev.. 2013; 16(4): 26-34. https://doi.org/10.32508/stdj.v16i4.1593
26. Tarım UA, Gürler1 O, Yalçın S. A Quick Method to Calculate NaI(Tl) Detector Efficiency Depending on Gamma ray Energy and Source-to-detector Distance. CBUJOS. 2018; 14(2): 195-199. https://doi.org/10.18466/cbayarfbe.396704
27. Ogundare FO, Oniya EO, Balogun FA. Dependence of NaI(Tl) detector intrinsic efficiency on source-detector distance, energy and off-axis distance:Their implications for radioactivity measurement. Pramana. 2008; 70: 863-874. https://doi.org/10.1007/s12043-008-0095-z
28. Jehouani A., Ichaoui R., Boulkheir M. Study of the NaI(Tl) efficiency by Monte Carlo method. Appl. Radiat Isot. 2000; 53(4-5): 887-891. https://doi.org/10.1016/S0969-8043(00)00254-2
29. Yavuzkanat N, Güngür D, Yalçın S. The Determination of the Total Efficiency for NaI(Tl) Detector by GATE Simulation. BEU J Sci. Technol.

2019; 8 (Special Issue): 37-45.https://doi.org/10.17798/bitlisfen.649129

30. Hu J, Liu F, Ouyang X. Monte Carlo Simulated the Detection Efficiency of Different H/R Ratio of NaI:TI Crystal. Appl Mech Mater.. 2014; 529: 391-394. https://doi.org/10.4028/www.scientific.net/AMM.529.391

نظام مصدر مشع – كاشف: التصميم و رأي مونت كارلو

زينب كريم علي ، علي نعمة محمد

قسم الفيزياء، كلية التربية، الجامعة المستنصرية، بغداد، العراق.

الخلاصة

تم في البحث الحالي تصميم و كتابة برنامج محاكاة حاسوبي وفقاً لطريقة مونت كارلو ليكون بمثابة نظام عملي إفتراضي بديلاً عن النظام الحقيقي. تم إختبار البرنامج إحصائياً و هندسياً وعددياً لنظام إفتراضي لمصدر مشع- كاشف. تم تنفيذ البرنامج لكاشف آيوديد الصوديوم ولعداد كايكر لمدى من الطاقة يصل إلى 10 MeV. تم استخدام قانون الأعداد الكبيرة (LLN) ونظرية النهاية المركزية (CLT) لاختبار دقة وضبط سير عمل البرنامج والإشارة إلى مدى قرب النتائج من متوسطاتها، وإحصائيًا، إلى أي مدى تميل إلى التوزيع الطبيعي. بشكل عام، أظهرت نتائج عدد من أنواع كفاءة الكاشف توافقاً كبيراً مع النتائج التجريبية المنشورة ونتائج عدد من البرامج العالمية ضمن نسبة خطأ 0,02-5% (أي دقة 95-99,98%) و بمستوى دلالة إحصائية يعكس إحكام خوارزمية المحاكاة. إن التخمين الدقيق والمضبوط للمحاكاة الحالية يمنحها الموثوقية المطلوبة. كما أظهر برنامج المحاكاة الحالي مرونة و فعالية عالية في تصميم أي نظام مصدر- كاشف نووي و تزويد العاملين أو المجربين ذات العلاقة بمؤشرات تساعد في التصميم الأمثل للمنظومة من حيث المكونات و هندسية النظام بأقل مدة زمنية. والتي قد تستغرق من بضعة ثواني الى بضعة دقائق لزمن تنفيذ بإستخدام حاسوب شخصي بمواصفات عادية. على عكس التجارب المختبرية التي قد تستغرق من عدة دقائق الى عدة ساعات. إضافة الى توفير بيئة عمل مثالية خالية من الإشعاع تماما". كما يقدم البرنامج الحالي فهماً عميقاً لما يحدث من تفاعلات في النظام الفيزيائي العملي الحقيقي.

الكلمات المفتاحية: نظرية النهاية المركزية، قانون الأعداد الكبيرة، ، طريقة مونت كارلو ، كفاءة كاشف آيوديد الصوديوم المطعّم بالثاليوم NaI(Tl)، احصائيات عد الاشعاع.